



Indocyanine green-loaded biodegradable nanoparticles: preparation, physicochemical characterization and in vitro release

Vishal Saxena^a, Mostafa Sadoqi^{b,*}, Jun Shao^a

^a Department of Pharmacy and Administrative Sciences, College of Pharmacy and Allied Health Professions,
St. John's University, 8000 Utopia Parkway, Jamaica, NY 11439, USA

^b Department of Physics, St. John's College of Liberal Arts and Sciences, St. John's University,
8000 Utopia Parkway, Jamaica, NY 11439, USA

Received 17 July 2003; received in revised form 6 January 2004; accepted 15 March 2004

Abstract

Purpose: The objective of this study is to develop indocyanine green (ICG)-loaded biodegradable nanoparticles by using biodegradable polymer, poly(DL-lactic-co-glycolic acid) (PLGA). **Method:** PLGA nanoparticles entrapping ICG were prepared by a modified spontaneous emulsification solvent diffusion method. To optimize the nanoparticle formulation, the influence of formulation parameters such as types of ICG, amount of ICG and the polymer were investigated. The ICG entrapment in nanoparticles, nanoparticle size and zeta potential were determined. The surface characterization was performed by atomic force microscopy (AFM) and the release of ICG from nanoparticles was determined. **Results:** All PLGA nanoparticle formulations were found to have the mean diameter within the range of 300–410 nm with polydispersity index (PI) within the range of 0.01–0.06. Indocyanine green showed more efficient entrapment as compared to indocyanine green sodium iodide salt. All indocyanine green-loaded nanoparticle formulations were found to have almost similar ICG content of nanoparticles and showed increase in ICG entrapment with increase in the amount of polymer. The ICG entrapment reached 74% when ICG: PLGA weight ratio in the formulation reached 1:800. AFM images indicated that the nanoparticles were almost spherical in shape and had numerous pores on their surfaces. The release pattern consisted of two phases, with initial exponential phase releasing about 78% of ICG (within 8 h) followed by a slow phase releasing about 2% of ICG (within next 16 h). **Conclusions:** ICG-loaded PLGA nanoparticles were prepared and the formulation was optimized. The increase in amount of polymer in formulation leads to higher ICG entrapment. Nanoparticles formed were spherical and had porous surfaces and exhibited the characteristic release pattern of a monolithic matrix based system.

© 2004 Elsevier B.V. All rights reserved.

Keywords: Indocyanine green; PLGA; Nanoparticles; Fluorescence; Near-infrared spectroscopy

1. Introduction

Indocyanine green (ICG) is a tricyanocyanine dye, which has been approved by the United States Food and Drug Administration for medical diagnostic studies, and is widely used for the evaluation of cardiac

* Corresponding author. Tel.: +1 718 990 1862;

fax: +1 718 990 5812.

E-mail address: sadoqim@stjohns.edu (M. Sadoqi).

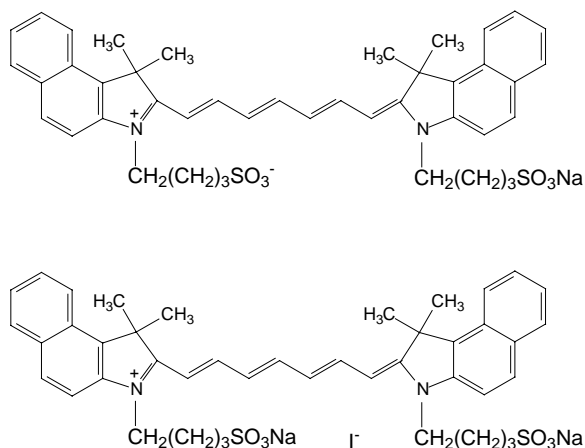


Fig. 1. Chemical structure of ICG (IR-125) (top) and ICG sodium iodide salt (ICG-NaI) (bottom).

output, liver function, microcirculation of skin flaps, visualization of the retinal and choroidal vasculatures, pharmacokinetic analysis, object localization in tissue, fluorescence probing of enzyme and proteins, tissue welding and photodynamic therapy, based on its fluorescing ability (Philip et al., 1996; Maarek et al., 2001). It absorbs and emits in the near-IR region of the spectrum. The chemical structure of ICG and ICG sodium iodide (ICG-NaI) is shown in Fig. 1.

Our previous investigations have proved that the degradation of ICG in aqueous solution followed first-order kinetics (Saxena et al., 2003). The degradation of ICG in aqueous solutions was accelerated by light exposure (photodegradation) (Saxena et al., 2003). Higher temperatures markedly accelerate the degradation of ICG in aqueous solutions (thermal degradation) (Saxena et al., 2003). Moreover, for quantitative analysis of ICG in aqueous solutions the effectiveness of steady state fluorescence technique has been demonstrated (Saxena et al., 2003). Since the degradation products of ICG fail to fluoresce in the wavelength region of ICG, the fluorescence signals obtained are directly proportional to the concentration of ICG in solution (Saxena et al., 2003).

ICG when administered intravenously has a plasma half-life of around 2–4 min and showed extensive protein binding (Mordon et al., 1998; Desmettre et al., 2000). The small circulation half-life and high protein binding of ICG in the body are major hur-

dles in its effective use as a fluorescence biomarker and photosensitizing agent, which requires long circulation half-life, targetability, accumulation at the tumor sites and prolong stay at the site of action. Thus, an injectable ICG formulation, with above mentioned qualities would be of great interest.

Earlier few studies have shown to increase the circulation half-life, residence time in the skin and confinement of ICG in the vascular compartment, by formulating an oil-in-water (O/W) ICG emulsion (Devoisselle et al., 1995; Mordon et al., 1997). Alternative approaches involve delivery systems for ICG, based upon biodegradable colloidal carriers. In recent years, polymeric nanoparticles (solid colloidal particles ranging from 1 to 1000 nm in size) have received considerable attention as a promising colloidal drug carrier (Soppimath et al., 2001). They have been widely used for controlled drug delivery via intravenous, ocular, and oral administration routes. Moreover, the nanoparticles have the ability to permeate the cells for cellular internalization and connective tissue permeation and thus deliver the drug efficiently to the targeted tissue without clogging the capillaries (Mu and Feng, 2003). The ability of nanoparticles to improve drug diffusion through biological barriers is a typical benefit for the delivery of biomarkers and photodynamic agents. The enhanced endocytotic activity and leaky vasculature in the tumor could result in accumulation of intravenously administered nanoparticles (Mu and Feng, 2003).

In recent years much attention has been focused on biodegradable polymers such as poly(DL-lactide-co-glycolide) (PLGA). PLGA have emerged as the most widely used and studied class of biodegradable polymers for pharmaceutical use due to their biocompatibility and biodegradability (Anderson and Shive, 1997). PLGA polymers have been approved by the United States Food and Drug Administration and have been used in humans for many years as a suture material. Various methods have been proposed for the preparation of PLGA nanoparticles (Fessi et al., 1989; Bodmeier and Cohen, 1990; Allemann et al., 1992). One promising technique is the spontaneous emulsification solvent diffusion (SESD) method (Niwa et al., 1993; Murakami et al., 1999), in which nano-sized particles (nanospheres) of PLGA can be effectively obtained by pouring the polymeric organic solution into an aqueous phase with moderate mechanical stir-

ring. Any drug or dye molecule added in the organic phase will be entrapped within the matrix type polymeric structure of these nanoparticles.

Therefore, the objective of our present study is to develop a polymeric nanoparticulate delivery system for ICG. For this purpose nanospheres of PLGA containing ICG were prepared by a modified spontaneous emulsification solvent diffusion method. The nanospheres preparations were fabricated in various recipes and the resulting products were characterized regarding their size, morphology and charge. In vitro drug release studies were also performed on the most promising formulation developed in this work. The techniques employed in characterization included the dynamic light scattering system (DLS) for the measurement of particle size and size distribution; electrophoretic light scattering system (ELS) for the measurement of zeta potential; atomic force microscopy (AFM) for morphological analysis; and steady state fluorescence spectroscopy for ICG encapsulation efficiency and in vitro release profile.

2. Materials and methods

2.1. Materials

Poly(DL-lactic-co-glycolic acid) (PLGA) 50:50 and polyvinyl alcohol (PVA) 88%–89% hydrolyzed were purchased from Sigma (Sigma Chemical Co., St. Louis, MO). Indocyanine green, free of sodium iodide (IR-25, laser grade) was obtained from Fisher Scientific (Fisher Scientific Inc., Pittsburgh, PA) and indocyanine green sodium iodide, ICG-NaI, (Diagnogreen[®] Injection) was obtained from Daiichi Pharmaceutical (Daiichi Pharmaceutical, Tokyo, Japan). All organic chemicals and solvents were of reagent grade. Distilled water was filtered by 0.22 μm syringe filter (Syrfil-MF Whatman Inc., Clifton, NJ) before use in the preparation process.

2.2. ICG-loaded PLGA nanoparticles preparation

In an attempt to optimize the nanoparticle formulation, the influences of various formulation parameters were investigated. Two different ICG forms (ICG-NaI and ICG), different ICG and polymer amounts used for

preparing the nanoparticle formulations were explored in various combinations. ICG-loaded PLGA nanoparticles were prepared by a modified spontaneous emulsification solvent diffusion method. Briefly, 8 ml of ICG solution in methanol was added to 16 ml of PLGA solution in acetonitrile to form a homogenous solution of PLGA and ICG. This homogenous solution was then added drop-wise into 120 ml aqueous PVA solution (pre-filtered through 0.22 μm filter), being stirred at 700 rpm by a laboratory magnetic stirrer. The nanoparticles suspension formed was then stirred for another 10 min at 700 rpm, followed by centrifugation for 20 min at 16,000 $\times g$. After centrifugation, the supernatant was discharged and the nanoparticle precipitate was then washed by using the same volume of distilled water as of the supernatant and again centrifuged at 16,000 $\times g$ for 6 min. The washing process was repeated three times. The washed nanoparticles were then freeze-dried using Freezone 4.5, freeze-drying system (Labconco, Kansas City, Missouri) for 36 h. The dried nanoparticles were stored at 0 $^{\circ}\text{C}$ in the dark until further use.

2.3. Indocyanine green assay

The concentrations of ICG were determined by steady-state fluorometry as reported earlier (Saxena et al., 2003) using a K-2 multifrequency cross-correlation phase and modulation fluorometer (ISS, Champaign, IL) equipped with a 70 mW cw diode laser. The diode laser had a wavelength of 786 nm, which was used as the excitation wavelength for all the studies. Emission spectra were recorded from 795 to 845 nm. Each measurement was performed in triplicate. A standard curve of ICG in dimethylsulfoxide (DMSO), having maximum concentration of 100 ng/ml was established with a linear regression coefficient of 0.999.

2.4. ICG entrapment efficiency, ICG content and nanoparticle recovery determination

The freeze-dried nanoparticles were weighed and dissolved in DMSO. Fluorescence spectrum of the solutions was measured. ICG concentrations were determined from the standard curve. ICG entrapment efficiency (%), ICG content in nanoparticles (% w/w) and nanoparticle recovery (%) were calculated by Eqs. (1),

(2) and (3), respectively.

ICG entrapment efficiency(%)

$$= \frac{\text{Mass of ICG in nanoparticles}}{\text{Mass of ICG used in formulation}} \times 100 \quad (1)$$

ICG content in nanoparticles(% w/w)

$$= \frac{\text{Mass of ICG in nanoparticles}}{\text{Mass of nanoparticles}} \times 100 \quad (2)$$

Nanoparticle recovery(%)

$$= \frac{\text{Mass of nanoparticles recovered}}{(\text{Mass of PLGA} + \text{Mass of ICG}) \text{ in formulation}} \times 100 \quad (3)$$

2.5. Characterization of nanoparticles

2.5.1. Particle size determination

Dynamic light scattering method was used to determine particle size using the particle size analyzer, NICOMP 380/DLS (Particle Sizing Systems Inc., Santa Barbara, CA). The dried nanoparticle samples were suspended in distilled water and were sonicated before measurement. The obtained homogeneous suspensions were examined to determine the mean diameter and polydispersity index. Each measurement was performed in triplicate.

2.5.2. Atomic force microscopy

The shape and surface morphology of the nanoparticles was determined by using atomic force microscope. The dried nanoparticle samples (Formulation 4, Table 1) were suspended in distilled water and were sonicated before measurement to obtain a homogeneous suspension. A drop of the nanoparticle suspension was mounted on the metal slabs, air-dried and was scanned by the atomic force microscope, Mul-

timode Scanning Probe Microscope (Digital Instruments, USA) maintained in a constant-temperature and vibration-free environment.

2.6. Surface charge

Nanoparticles were characterized with respect to zeta (ζ) potential by using zeta potential analyzer, NICOMP 380/ZLS (Particle Sizing Systems Inc., Santa Barbara, CA). The dried nanoparticle samples were suspended in distilled water (pH 7) and were sonicated before measurement. The obtained homogeneous suspensions were examined to determine the zeta (ζ) potential.

2.7. In vitro release study

The release pattern of ICG from the nanoparticles was determined in phosphate buffer saline, PBS (pH 7.4) under sink conditions, in triplicate. The amount of ICG remaining in the nanoparticles after a certain time period was obtained by measuring steady state fluorescence of ICG from the nanoparticles. Briefly, a known quantity of nanoparticles was suspended in the buffer solution and was sonicated to get a homogenous suspension. This suspension was filled in three microcentrifuge tubes and was kept in Dubnoff metabolic shaking incubator (Precision, Winchester, VA) maintained at 37 °C and shaken horizontally at 80 min⁻¹. At a certain time point, for the measurement of fluorescence from the nanoparticles the tubes were taken out of the shaking incubator and centrifuged at 14,000 rpm for 2 min. The supernatant was removed and the precipitated nanoparticles at the bottom of the tubes were resuspended in 2 ml of fresh buffer by sonication. Then the steady state fluorescence measurement of this fresh suspension was performed. The cumulative

Table 1

Affect of formulation parameters on ICG entrapment efficiency, ICG content and nanoparticle recovery

| Formulation number | Amount of ICG in formulation (mg) | Amount of polymer in formulation (mg) | ICG content (%) ^a | ICG entrapment (%) ^a | Nanoparticle recovery (%) |
|--------------------|-----------------------------------|---------------------------------------|------------------------------|---------------------------------|---------------------------|
| 1 | 1 | 100 | 0.21 ± 0.06 | 9.92 ± 2.68 | 48.0 |
| 2 | 5 | 100 | 0.29 ± 0.04 | 2.92 ± 0.40 | 49.4 |
| 3 | 10 | 100 | 0.17 ± 0.01 | 1.14 ± 0.08 | 65.3 |
| 4 | 1 | 800 | 0.20 ± 0.00 | 74.47 ± 0.74 | 45.7 |

^a n = 3.

percentage of ICG released from the nanoparticles at a certain time point was obtained using Eq. (4).

$$\begin{aligned} \text{Cumulative\% ICG released} \\ = 100 - \text{\%ICG remaining} \end{aligned} \quad (4)$$

3. Results and discussion

3.1. Formulation optimization

Structurally, ICG has a complex molecular structure (Fig. 1), having two polycyclic parts imparting lipophilic character and a sulfate group bound to each polycyclic part, imparting hydrophilic character to the molecule. Thus, ICG shows solubility in various organic solvents such as DMSO, methanol, acetonitrile etc. and in aqueous solvents such as water, PBS etc. This amphiphilic nature of ICG is one of the major hurdles in formulating a nanoparticle formulation with PLGA to entrap ICG. Due to its water-solubility the ICG molecules quickly partition out into the water phase from the organic phase during the solvent emulsification and diffusion process, leading to low ICG entrapment.

When ICG-NaI was used in preparing nanoparticle formulation, very low ICG entrapment and ICG content of the nanoparticles were obtained (data not shown). This was mainly due to relatively more hydrophilic nature of the ICG-NaI molecule, which caused extremely less ICG retention in the polymer matrix. So, ICG-NaI was excluded from further formulations. On the other hand, in the case of ICG (IR-125) sufficient ICG entrapment and ICG content of nanoparticles was observed. This was probably due to its relatively less hydrophilic nature as compared to ICG-NaI, which enabled ICG to be retained in the hydrophobic nanoparticle matrix.

To increase the drug loading in the nanoparticles, the amount of ICG in the formulations was varied from 1 to 10 mg and the amount of polymer was varied from 100 to 800 mg. The results (Table 1) showed that in formulation number 1–3, when the initial amount of ICG used in the formulations was increased while maintaining the amount of the polymer in the formulation constant there is a decrease in ICG entrapment in the nanoparticles. Whereas, in the formulation number 1 and 4, when the amount of polymer was increased by

eight times, while keeping the amount of ICG constant, ICG entrapment was increased almost eight times. For all the formulations, the ICG content of the nanoparticles (% w/w) were nearly constant. This reflected that PLGA nanoparticles have a fixed capacity to entrap high hydrophilic ICG molecules. As the polymer amount was increased ICG entrapment increased, due to the availability of more polymer (nanoparticles) to entrap the same amount of ICG molecules. One of the goals of this study was to obtain nanoparticulate formulation of ICG with optimal properties in terms of size integrity, drug loading, entrapment efficiency and to minimize drug loss during the nanoparticle preparation. The nanoparticles from formulation number 4 were used for surface morphology and in vitro release studies.

3.2. Size and size distribution

The average mean diameter and polydispersity of all nanoparticle samples were determined and are listed in Table 2. The nanoparticles mean diameters from all the formulations were very close and were in the range of 305–405 nm. For all nanoparticle formulations obtained, the polydispersity index (PI) was in the range of 0.01–0.06, which indicated a narrow particle size distribution. The ICG entrapment into the nanoparticles did not significantly affect particle size, and moreover, no direct correlation can be obtained between ICG content and nanoparticle size.

3.3. Surface charge

The results of zeta (ζ) potential measurements are reported in Table 2. For all the formulations, the nanoparticles exhibited similar low zeta potentials ranging from -7.2 to -16.3 mV. Generally,

Table 2
Size and zeta potential (ζ) values of various nanoparticle formulations

| Formulation number | Nanoparticle size (nm) ^a | Polydispersity | Zeta potential (mV) ^a |
|--------------------|-------------------------------------|----------------|----------------------------------|
| 1 | 405 ± 0.05 | 0.01 | -7.2 ± 1.0 |
| 2 | 338 ± 0.12 | 0.04 | -7.8 ± 0.8 |
| 3 | 307 ± 0.08 | 0.02 | -10.3 ± 2.1 |
| 4 | 357 ± 0.21 | 0.06 | -16.3 ± 1.5 |

^a ($n = 3$).

high negative zeta potential values are expected for pure polyester nanoparticles due to the presence of carboxyl groups on the polymeric chain extremities (Konan et al., 2003). However, in this investigation the zeta potential values are close to zero. The factor which might be responsible for such an effect can be the presence of residual PVA on the nanoparticle surface. The presence of residual PVA on the nanoparticle surface has been determined by other authors (Konan et al., 2003). The residual PVA on the nanoparticle surface can create a shield between the nanoparticle surface and the surrounding medium (Konan et al., 2003). Moreover, PVA would mask the possible charged groups existing on the particle surface leading to zeta potential values close to zero (Konan et al., 2003).

3.4. Morphology

Fig. 2 represents a three dimensional image of the nanoparticles, obtained by AFM. The nanoparticles were nearly spherical in shape. The nanoparticles size values obtained from the image matches well with

the size range obtained by dynamic light scattering. Fig. 3 shows the surface morphology of the nanoparticles. This image clearly shows the numerous pores on the surface of the nanoparticles. The pores sizes as shown in the figure ranges from 9 to 22 nm. This porous nature of the nanoparticle surface is the major characteristics of PLGA nanoparticles responsible for the controlled release of entrapped materials from the nanoparticles.

Also, Fig. 3 shows the presence of a discontinuous layer of some material on the surface of the nanoparticles. These surface patches might represent either ICG molecules adsorbed or entangled on the surface of the nanoparticles or residual PVA layer present on the nanoparticle surface. Further studies are needed to be performed in order to establish the exact nature of this surface layer.

3.5. Release profile of ICG

In our previous investigations we had shown that ICG degrades in aqueous media and undergoes considerable photo and thermal degradation (Saxena et al.,

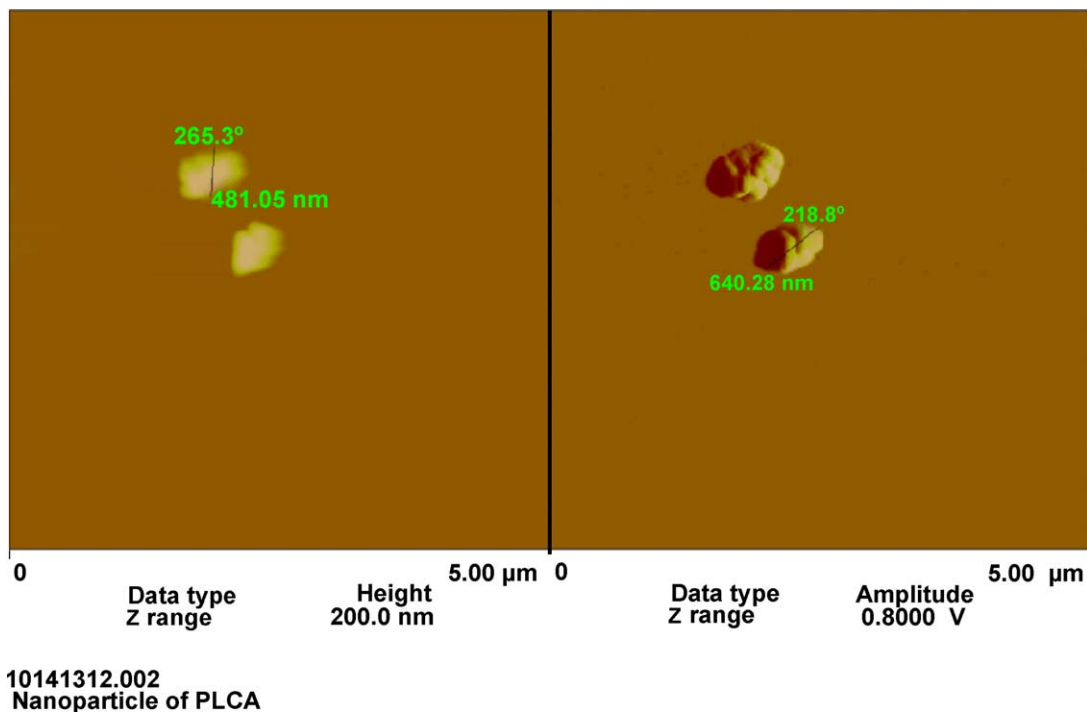


Fig. 2. Atomic force microscopy images of ICG-loaded PLGA nanoparticles.

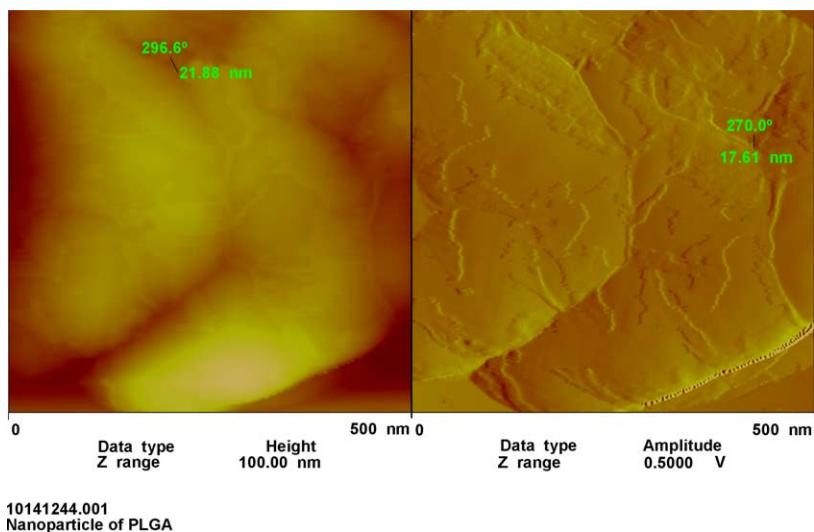


Fig. 3. Surface characterization of ICG-loaded PLGA nanoparticles (Formulation 4 of Tables 1 and 2).

2003). Therefore, to obtain the release profile of ICG from the nanoparticles, the conventional sampling and measurement of ICG in the supernatant (obtained after centrifugation of the nanoparticle sample) or release media was not utilized. Our studies with ICG-loaded PLGA nanoparticles had shown that nanoparticle entrapment reduced the degradation of ICG to a great extent in aqueous media along with efficient photostabilization and thermal stabilization of ICG (Saxena et al., 2004). We hypothesized that this stability of ICG in nanoparticles in aqueous media is due to its entrapment within the nanoparticle matrix, and once ICG is released out from the nanoparticles into the aqueous media, its degradation takes place. Thus, a

new method based on measuring the amount of ICG left in the nanoparticles after a particular time interval was utilized in the present study.

Fig. 4 represents the release profile of ICG from ICG-loaded PLGA nanoparticles. ICG release from the nanoparticles appeared to have two components. First an initial exponential phase releasing 78% of ICG (within 8 h) followed by a slow phase releasing up to 80% of ICG (within next 16 h). The initial exponential release phase of ICG was probably due to ICG which was adsorbed or close to the surface of the nanoparticles and due to diffusion of the dissolved ICG within the PLGA core of the nanoparticle into the release medium. The large surface to volume ratio

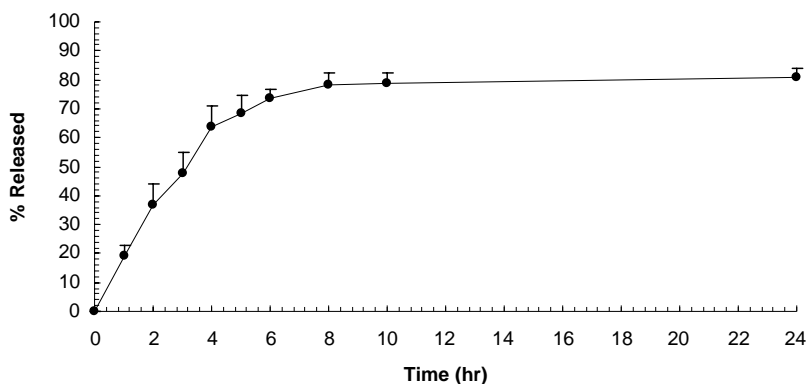


Fig. 4. The release profile of ICG from ICG-loaded PLGA nanoparticles ($n = 3$).

of the nanoparticle geometry and the water-soluble nature of ICG can be the contributing factors for the initial release pattern of ICG from ICG-loaded PLGA nanoparticles. The exponential type of release pattern for PLGA nanoparticles have been reported by several authors (Govender et al., 1999; Jeon et al., 2000).

4. Conclusion

The present research proposed a novel nanoparticulate formulation for ICG by entrapping ICG within PLGA polymeric matrix. Investigations on the preparation, characterization and in vitro release of the nanoparticles were carried out. The different formulations with different types of ICG, amounts of ICG and polymer were evaluated and optimized. The results indicated that ICG is the better candidate for entrapment within the PLGA nanoparticles as compared to its sodium iodide salt (ICG-NaI). ICG can be entrapped into PLGA nanoparticles with high entrapment efficiencies. Within the bounds of formula variation tested, the ICG-loaded nanoparticles exhibited the similar characteristics in terms of ICG content of nanoparticles, particle size and surface characteristics. The produced nanoparticles were nearly spherical in shape with porous surfaces. The release profile of the nanoparticles consists of two distinct phases, an initial exponential phase followed by a slow release phase, representing characteristic of monolithic matrix based systems.

Acknowledgements

The authors are very grateful to Professor Kalle Levon, Polytechnic University, NY for his assistance with Atomic Force Microscopy and Professor Sunil Kumar, Polytechnic University, NY for his scientific inputs and help in reviewing this manuscript. We also thank Professor Kwon Ho Kim, St. John's University, NY for his valuable discussions.

References

Allemann, E., Gurny, R., Doelker, E., 1992. Preparation of aqueous polymeric nanodispersions by a reversible salting-out process,

- influence of process parameters on particle size. *Int. J. Pharm.* 87, 247–253.
- Anderson, J.M., Shive, M.S., 1997. Biodegradation and biocompatibility of PLA and PLGA microspheres. *Adv. Drug Del. Rev.* 28, 5–24.
- Bodmeier, R., Cohen, H., 1990. Indomethacin polymeric nanosuspension prepared by microfluidization. *J. Controlled Rel.* 12, 1 223–233.
- Desmettre, T., Devoisselle, J.M., Mordon, S., 2000. Fluorescence properties and metabolic features of indocyanine green (ICG) as related to angiography. *Surv. Ophthalmol.* 45, 15–27.
- Devoisselle, J.M., Soulie, S., Mordon, S.R., Mestres, G., Desmettre, T., Maillols, H., 1995. Effect of indocyanin green formulation on blood clearance and in vivo fluorescence kinetic profile of skin. *Proc. SPIE Opt. Biopsies* 2627, 100–108.
- Fessi, H., Puisieux, F., Devissaguet, J.P., Ammoury, N., Benita, S., 1989. Nanocapsule formation by interfacial polymer deposition following solvent displacement. *Int. J. Pharm.* 55, R1–R4.
- Govender, T., Stolnik, S., Garnett, M.C., Illum, L., Davis, S.S., 1999. PLGA nanoparticles prepared by nanoprecipitation: drug loading and release studies of a water soluble drug. *J. Controlled Rel.* 57, 171–185.
- Jeon, H.J., Jeong, Y.I., Jang, M.K., Park, Y.H., Nah, J.W., 2000. Effect of solvent on the preparation of surfactant-free poly(DL-lactide-co-glycolide) nanoparticles and norfloxacin release characteristics. *Int. J. Pharm.* 207, 99–108.
- Konan, Y.N., Cerny, R., Favet, J., Berton, M., Gurny, R., Allemann, E., 2003. Preparation and characterization of sterile sub-200 nm meso-tetra(4-hydroxylphenyl) porphyrin-loaded nanoparticles for photodynamic therapy. *Eur. J. Pharm. Biopharm.* 55, 115–124.
- Maarek, J.M.I., Holschneider, D.P., Harimoto, J., 2001. Fluorescence of indocyanine green in blood: intensity dependence on concentration and stabilization with sodium polyaspartate. *J. Photochem. Photobiol. B: Biol.* 65, 157–164.
- Mordon, S., Desmettre, T., Devoisselle, J.M., Mitchell, V., 1997. Selective laser photocoagulation of blood vessels in a hamster skin flap model using a specific ICG formulation. *Laser Surg. Med.* 21, 365–373.
- Mordon, S., Devoisselle, J.M., Soulie-Begu, S., Desmettre, T., 1998. Indocyanine green: physicochemical factors affecting its fluorescence in vivo. *Microvasc. Res.* 55, 146–152.
- Mu, L., Feng, S.S., 2003. A novel controlled release formulation for the anticancer drug paclitaxel (Taxol®): PLGA nanoparticles containing vitamin E TPGS. *J. Controlled Rel.* 86, 33–48.
- Murakami, H., Kobayasi, M., Takeuchi, H., Kawashima, Y., 1999. Preparation of poly(DL-lactide-co-glycolide) nanoparticles by modified spontaneous emulsification solvent diffusion method. *Int. J. Pharm.* 187, 143–152.
- Niwa, T., Takeuchi, H., Hino, T., Kunou, N., Kawashima, Y., 1993. Preparation of biodegradable nanospheres of water-soluble and insoluble drugs with D,L -lactide/glycolide copolymer by a novel spontaneous emulsification solvent diffusion method, and the drug release behavior. *J. Controlled Rel.* 25, 89–98.
- Philip, R., Penzkofer, A., Baumler, W., Szeimies, R.M., Abels, C., 1996. Absorption and fluorescence spectroscopic investigation of indocyanine green. *J. Photochem. Photobiol. A: Chem.* 96, 137–148.

- Saxena, V., Sadoqi, M., Shao, J., 2003. Degradation kinetics of indocyanine green in aqueous solution. *J. Pharm. Sci.* 92, 2090–2097.
- Saxena, V., Sadoqi, M., Shao, J., 2004. Enhanced photo-stability, thermal-stability and aqueous-stability of Indocyanine green in polymeric nanoparticulate systems. *J. Photochem. Photobiol. B: Biol.* 74, 29–38.
- Soppimath, K.S., Aminabhavi, T.M., Kulkarni, A.R., Rudzinski, W.E., 2001. Biodegradable polymeric nanoparticles as delivery devices. *J. Controlled Rel.* 70, 1–20.